Proceedings of the ASME 2023
International Design Engineering Technical Conferences and
Computers and Information in Engineering Conference
IDETC-CIE2023
August 20-23, 2023, Boston, Massachusetts

DETC2023-116669



# INTRODUCTION OF LOCAL RESONATORS TO A NONLINEAR METAMATERIAL WITH TOPOLOGICAL FEATURES

**Arun Malla**[*], **Joshua LeGrande**[*], **Mohammad Bukhari**, **Oumar Barry**[†]
Department of Mechanical Engineering
Virginia Polytechnic Institute and State University
Blacksburg, Virginia 24061

## ABSTRACT

*Metamaterials have been shown to benefit from the addition of local resonators, nonlinear elements, or topological properties, gaining features such as additional bandgaps and localized vibration modes. However, there is currently no work in the literature that examines a metamaterial system including all three elements. In this work, we model a 1-dimensional metamaterial lattice as a spring-mass chain with coupled local resonators. Quasiperiodic modulation in the nonlinear connecting springs is utilized to achieve topological features. For comparison, a similar system without local resonators is also modeled. Both analytical and numerical methods are used to study this system. The infinite chain response of the proposed system is solved through the perturbation method of multiple scales. This analytical solution is compared to the finite chain response, estimated using the method of harmonic balance and solved numerically. The resulting band structures and mode shapes are used to study the effects of quasiperiodic parameters and excitation amplitude on the system behavior both with and without the presence of local resonators. Specifically, the impact of local resonators on topological features such as edge modes is established, demonstrating the appearance of a trivial bandgap and multiple localized edge states for both main cells and local resonators.*

## 1 INTRODUCTION

Metamaterials are artificial engineered structures that are patterned with special configurations and material constituents [1–3]. These structures possess properties not found in naturally occurring materials, ranging from zero or negative values of standard engineering parameters (such as density and Poisson's ratio [1]), to nonlinear phenomena (such as gap solitons [4] and asymmetric wave propagation [5]). Metamaterials have a foundation in optics and electromagnetics, exploiting elastic and wave properties such as motion, deformations, stresses and mechanical energy [6, 7]. These concepts were later extended for elastic wave propagation [2] and acoustics [8]. The unusual features of metamaterials make them beneficial for numerous applications including vibration and noise control, energy harvesting, health monitoring, and acoustic diodes or rectifiers. Within elastic media, metamaterials are usually patterned in periodic (phononic), quasiperiodic, or random structural configurations [9]. It was observed that periodic structures prevent waves from propagating through the structure at certain frequency ranges, known as bandgaps, through a phenomenon known as Bragg scattering. Therefore, low frequency waves can be banned from propagating through the structure, thus achieving significant vibration attenuation [2, 10]. However, since the Bragg scattering is restricted to certain lattice constants, only large structures can be controlled.

This large structure requirement can be counteracted by introducing local resonators into metamaterials [11]. Thus, applications of vibration attenuation can be extended to much smaller structures and applications. Local resonators are also capable of

[*]These authors contributed equally to this work.
[†]Corresponding Author (Email: obarry@vt.edu)

widening the original bandgap developed by Bragg scattering, as the bandgap is directly influenced by the resonator parameters [12]. Furthermore, by introducing multiple resonators, additional bandgaps can be obtained [13, 14].

In addition, nonlinear elements can also be included in a metamaterial [15]. On top of the potential for improved bandgap performance, the introduction of nonlinear elements also results in other interesting wave propagation phenomena such as gap solitons [16], dark and enveloped solitons [17], cloaking [18–20], and wave nonreciprocity [21–23]. These phenomena can be applied for a host of applications. One option for the addition of nonlinearity to the metamaterial system is the use of nonlinear springs. These springs can have a combined linear and nonlinear stiffness or be essentially nonlinear, with nonlinear stiffness only. In the literature, study of nonlinear metamaterials is often focused on obtaining the band structure analytically or numerically [24, 25]. The former uses perturbation techniques (such as Lindstedt–Poincare [26], multiple scales [27] and homotopy analysis [28]), while the latter applies frequency and spectro-spatial analysis [29–32].

Quasiperiodic arrangements have also been shown to improve energy harvesting and vibration control through topologically protected modes. The investigation of topological phases of matter in metamaterials has shown the presence of robust topologically protected modes that do not propagate inside the bulk and are localized within lower dimensions [33]. One passive method for manifesting these topological modes is the breaking of spatial inversion symmetry while maintaining time-reversal symmetry [34–36]. This can be achieved by introducing quasiperiodic modulation into a structure using patterns such as the Aubry-André model as seen in [37–40]. This results in a spectrum that is analogous to the Hofstadter butterfly [41] with additional nontrivial topological bandgaps inside the bulk of propagating waves in periodic structures. These topological bandgaps host localized modes that can be beneficial in vibration mitigation [42] showing high displacement in a few cells while preventing wave propagation to other cells. Localization can also be moved along the metamaterial by topological pumping [43].

Further investigations have been made studying the effects of nonlinearity on topological metamaterials. The majority of these studies generally fall into one of two paths. The first path observes the effect of nonlinearity on a metamaterial that is topological in the linear regime. The second uses nonlinearity to strategically design metamaterials to induce topological properties in the metamaterial. In both cases, the amplitude dependence of the nonlinear response has led to studies in the frequency shift [44–46] and stability [47, 48] of topological edge states. One most common result of combining topological and nonlinear effects is the existence of solitons that are topologically robust [49–51].

In this paper, we examine a metamaterial system with local resonators, nonlinear springs, and quasiperiodic patterning. Previous works have examined each of these features, with a nonlinear metamaterial with local resonators being studied by Bukhari et al. [32] and a nonlinear quasiperiodic system being studied by Rosa at al. [52]. This paper expands the latter work to include local resonators and investigates the resulting effects on vibration propagation in both the linear and nonlinear regimes. The system consists of a spring-mass chain with coupled local resonators and quasiperiodicity in the nonlinear connecting springs. The infinite chain model is solved analytically using the method of multiple scales, providing a closed form solution for the slow flow equations and nonlinear frequency correction factor. The method of harmonic balance is used to numerically estimate the behavior of a finite chain, providing insight into the natural frequencies and mode shapes of both main cells and local resonators. Both these methods are used to study the effects of quasiperiodic parameters and excitation amplitude on the system behavior, focusing on the potential for vibration localization and control. The system is compared to the previously studied system lacking resonators, and the effect of local resonators on topological edge states and the behavior of local resonators in the proposed nonlinear quasiperiodic system is examined.

## 2 MODELING AND SOLUTION METHODS

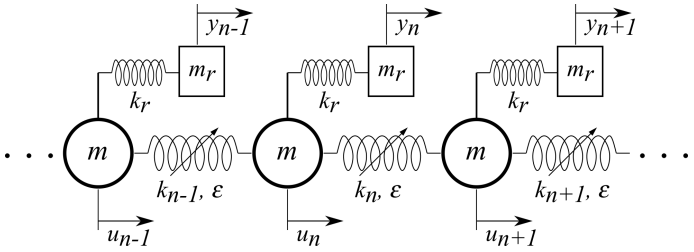


**FIGURE 1**: Schematic of nonlinear, quasiperiodic chain with local resonators.

This work considers a 1-dimensional nonlinear locally resonant metamaterial with stiffness modulation in the main springs as shown in Fig. 1. The metamaterial is represented by a spring mass chain of identical masses, $m$, joined by modulated springs with linear and cubic nonlinear components. Each mass is coupled to a local resonator with mass, $m_r$ and stiffness, $k_r$. Modulation in the main springs follows the Aubry-André Model such that the stiffness constant between mass $n$ and mass $n+1$ is defined as

$$k_n = k_0[1 + \lambda cos(2\pi n\theta + \phi)] \tag{1}$$

with average stiffness, $k_0$, and modulation amplitude, $\lambda$. This pattern is defined by its quasiperiodic parameter, $\theta$, and phase shift, $\phi$. It should be noted that $|\lambda| < 1$ in order to avoid negative

values of stiffness $k_n$. Rational and irrational values of $\theta$ produce periodic and quasiperiodic patterns, respectively. The governing equations of motion for the $n^{\text{th}}$ mass and resonator are

$$m\ddot{u}_n + k_{n-1}(u_n - u_{n-1}) + k_n(u_n - u_{n+1}) + k_r(u_n - y_n) + \varepsilon k_{n-1}(u_n - u_{n-1})^3 + \varepsilon k_n(u_n - u_{n+1})^3 = 0 \quad (2)$$

$$m_r\ddot{y}_n + k_r(y_n - u_n) = 0 \quad (3)$$

where $u_n$ and $y_n$ are the displacements of the $n^{\text{th}}$ mass and resonator, respectively, and $\varepsilon$ is a small dimensionless parameter defining the strength of the nonlinearity. These equations can be expressed compactly in matrix form for the $j^{\text{th}}$ unit cell as

$$\mathbf{M}\ddot{\mathbf{u}}_j + \mathbf{K}_{(0)}\mathbf{u}_j + \mathbf{K}_{(-1)}\mathbf{u}_{j-1} + \mathbf{K}_{(1)}\mathbf{u}_{j+1} + \varepsilon\mathbf{f}^{NL} = 0 \quad (4)$$

where for a system with $q$ masses in its unit cell, $\mathbf{M}$, $\mathbf{K}_{(0)}$, $\mathbf{K}_{(-1)}$, and $\mathbf{K}_{(1)}$ are $2q \times 2q$ mass and stiffness matrices, $\mathbf{u}_j$ is the $2q \times 1$ vector of mass and resonator displacements, and $\mathbf{f}^{NL}$ is the $2q \times 1$ nonlinear forcing vector.

## 2.1 THE METHOD OF MULTIPLE SCALES

To derive the dispersion relation for an infinite chain, the perturbation method of multiple scales (MMS) is utilized with the fast time scale, $T_0 = t$, and the slow time scale, $T_1 = \varepsilon t$. We can assume expansions for the displacements in the form of

$$\mathbf{u}_j = \mathbf{u}_j^{(0)}(T_0, T_1) + \varepsilon\mathbf{u}_j^{(1)}(T_0, T_1) + O(\varepsilon^2) \quad (5)$$

and the time derivative can be expressed as

$$\frac{\partial^2}{\partial t^2} = D_0^2() + 2\varepsilon D_0 D_1() + O(\varepsilon^2) \quad (6)$$

where $D_n = \partial/\partial T_n$.

Using these expansions, the equation of motion can be broken into linear and nonlinear components by order of $\varepsilon$ yielding order $\varepsilon^0$

$$D_0^2\mathbf{M}\mathbf{u}_j^{(0)} + \mathbf{K}_{(0)}\mathbf{u}_j^{(0)} + \mathbf{K}_{(-1)}\mathbf{u}_{j-1}^{(0)} + \mathbf{K}_{(1)}\mathbf{u}_{j+1}^{(0)} = 0 \quad (7)$$

order $\varepsilon^1$

$$D_0^2\mathbf{M}\mathbf{u}_j^{(1)} + \mathbf{K}_{(0)}\mathbf{u}_j^{(1)} + \mathbf{K}_{(-1)}\mathbf{u}_{j-1}^{(1)} + \mathbf{K}_{(1)}\mathbf{u}_{j+1}^{(1)} = -2D_0D_1\mathbf{M}\mathbf{u}_j^{(0)} - \mathbf{f}^{NL} \quad (8)$$

At order $\varepsilon^0$, the problem is linear, so the solution can be expressed as

$$\mathbf{u}_j^{(0)} = \frac{1}{2}A(T_1)\psi e^{i(\mu j - \omega_0 T_0)} + c.c. \quad (9)$$

where $A$ is the amplitude, $\psi$ is the mode shape, $\mu$ is the dimensionless wavenumber, $\omega_0$ is the linear natural frequency, and $c.c.$ denotes the complex conjugate. Substituting the solution into the linear equation yields the linear eigenvalue problem

$$\omega_0^2\mathbf{M}\psi = \mathbf{K}(\mu)\psi \quad (10)$$

where

$$\mathbf{K}(\mu) = \mathbf{K}_{(0)} + \mathbf{K}_{(-1)}e^{-i\mu} + \mathbf{K}_{(1)}e^{i\mu} \quad (11)$$

the solution of which obtains the linear dispersion relation and eigenvectors of the system.

Looking now to the nonlinear problem (i.e., the order $\varepsilon$ problem), Eq. 8 is decoupled through the use of modal coordinates, then non-secular terms are isolated to derive the slow flow equations. Next, we introduce the polar form of the displacement amplitude

$$A_n = \alpha_n(T_1)e^{-i\beta_n(T_1)} \quad (12)$$

For a trimer lattice with $\theta = 1/3$, the slow flow equations are then solved to yield

$$\alpha_n' = 0 \quad (13)$$

$$\beta_n' = \frac{3\alpha_n^2 c_n(\mu)}{8m\omega_{0,n}\eta_n} \quad (14)$$

where

$$\begin{aligned} c_n(\mu) = &-2k_3\bar{\psi}_1\psi_3(|\psi_1|^2 + |\psi_3|^2)e^{-i\mu} + k_3\bar{\psi}_1^2\psi_3^2e^{-2i\mu} \\ &+k_3\bar{\psi}_3^2\psi_1^2e^{2i\mu} - 2k_3\bar{\psi}_3\psi_1(|\psi_1|^2 + |\psi_3|^2)e^{i\mu} \\ &+(k_1+k_3)|\psi_1|^4 + (k_1+k_2)|\psi_2|^4 + (4k_1|\psi_2|^2 \\ &+4k_3|\psi_3|^2 - 2k_1(\bar{\psi}_1\psi_2 + \bar{\psi}_2\psi_1))|\psi_1|^2 + (k_2+k_3)|\psi_3|^4 \\ &+(4k_2|\psi_3|^2 - 2k_1\bar{\psi}_1\psi_2 - (2k_1\psi_1 + 2k_2\psi_3)\bar{\psi}_2 \\ &-2k_2\psi_2\bar{\psi}_3)|\psi_2|^2 - 2k_2(\bar{\psi}_2\psi_3 + \bar{\psi}_3\psi_2)|\psi_3|^2 \\ &+k_1\bar{\psi}_1^2\psi_2^2 + (k_1\psi_1^2 + k_2\psi_3^2)\bar{\psi}_2^2 + k_2\bar{\psi}_3^2\psi_2^2 \end{aligned} \quad (15)$$

and

$$\eta_n = |\psi_1|^2 + |\psi_2|^2 + |\psi_3|^2 + \sqrt{\frac{m}{m_r}}(|\psi_4|^2 + |\psi_5|^2 + |\psi_6|^2) \quad (16)$$

with $\psi_n$ being the $n^{\text{th}}$ element of the eigenvector associated with wavenumber, $\mu$, and $\bar{\psi}_n$ being its complex conjugate. It can be shown that $c_n$ is a purely real quantity.

The solution further allows us to express the nonlinear frequency in terms of the frequency correction factor, $\beta_n'$ as

$$\omega_n = \omega_{0,n} + \varepsilon\beta_n' \tag{17}$$

## 2.2 THE METHOD OF HARMONIC BALANCE

While the method of multiple scales provides the dispersion relations for an infinite chain, this solution may not reflect certain important aspects, such as the presence of topological edge modes [52]. To examine these modes, a finite chain of $N = 42$ cells with free boundary conditions at each end is studied using the harmonic balance method [45, 52]. This method allows us to estimate the mode shapes and natural frequencies of the finite system for varying excitation amplitude.

Beginning with the equations of motions in Eqs. 2 and 3, periodic solution forms for the displacement of the main cell and resonator masses are assumed as

$$u_n = a_n \cos(\omega t) + b_n \sin(\omega t) \tag{18}$$

$$y_n = c_n \cos(\omega t) + d_n \sin(\omega t) \tag{19}$$

where $a_n, b_n, c_n, d_n$ are unknown displacement coefficients. $\omega = 2\pi/T$ is the unknown assumed angular frequency with period $T$, resulting in $4N+1$ unknowns.

A corresponding set of $4N+1$ nonlinear equations are obtained by substituting Eqs. 18 and 19 into the governing equations of motion, then setting the coefficient terms of $\cos(\omega t)$ and $\sin(\omega t)$ to 0. The final equation is provided by setting the $L_2$ norm of the displacement coefficients, $\mathbf{x} = \{a_1, b_1, c_1, d_1, ..., a_N, b_N, c_N, d_N\}^T$, equal to the total chain amplitude $A$.

$$\|\mathbf{x}\|_2 = A \tag{20}$$

For comparison to the infinite chain in the MMS solution, chain amplitude $A$ is also used to define the Bloch wave amplitude, $\alpha_n$, by $\alpha_n = A/\sqrt{\theta N}$. This is to ensure that when the wave solution is extended to a finite lattice with $N$ masses, the resulting $L_2$ norm is equal to $A$ [52].

The described set of $4N+1$ algebraic nonlinear equations are solved numerically using a trust-region algorithm through MATLAB's "fsolve" function. To investigate the amplitude dependant effects of nonlinearity, the amplitude is first set to a small value, $A = 10^{-3}$. The initial guess for this case is the solution to the linear problem. Following this, $A$ is increased in small increments, with each increase using the previous solution as the initial guess. Thus, the displacements and frequencies of the finite chain are calculated for a range of $A$.

# 3 RESULTS

Using the previously described solution methods, we examine selected variations of the proposed metamaterial. In this study, we consider a trimer lattice ($\theta = 1/3$) with the following parameters: $m = 1$ kg, $k_0 = 1$ N/m, $\lambda = 0.6$, $m_r = 0.2$ kg, $k_r = 0.3$ N/m, and $\varepsilon = 0.1$. Although the system is only quasiperiodic for irrational $\theta$ values and periodic for rational $\theta$ values, the dispersion relations depend continuously on $\theta$ and can be accurately represented through sampling over rational values of $\theta$. Several cases are studied, specifically a chain with linear springs or nonlinear springs, and with resonators or without resonators. While the linear dispersion relation will be given for a full range of phase variable, $\phi$, the nonlinear dispersion relation will be given only for $\phi = 0.35\pi$ as more attention is given to its amplitude dependence than its phase dependence. Thus, the nonlinear dispersion relation is determined for varying displacement amplitudes, $A$, with set $\phi$.

## 3.1 BAND STRUCTURE

The dispersion relations are shown in Fig. 2 for linear and nonlinear systems with and without resonators. The bulk bands for an infinite chain, modeled from the unit cell and solved via MMS, are shown in blue. The natural frequencies of a finite chain, modeled with 42 masses and solved by harmonic balance, are overlaid as black lines. Comparing Fig. 2(a) and (b), the presence of the resonators in the linear chain has expected effects on the band structure as seen in previous studies [39, 40]. The dispersion band is split in two by a topologically trivial bandgap centered on the resonant frequency of the resonators. Above and below this bandgap, both bands are split into additional bands by topologically nontrivial bandgaps, resulting in a total of 6 bands compared to the 3 bands of the non-resonator case. The location and number of these nontrivial bandgaps are determined by the quasiperiodic parameter. Both with and without resonators, the frequencies of the finite chain reveal the presence of edge states that span the bandgaps. The frequency of these edge states is dependant on $\phi$ for the linear chain. Observing the case with resonators in Fig. 2(b) confirms that these edge states are present for nontrivial bandgaps only.

To observe the amplitude dependence, the nonlinear dispersion is plotted with increasing amplitude for the chains without and with resonators in Fig. 2(c) and (d) respectively. As in the linear case, the presence of resonators introduces a trivial bandgap, with nontrivial bandgaps on either side. In the nonlinear regime, frequencies shift upward with increasing amplitude for a positive nonlinearity ($\varepsilon = 0.1$). This effects several bandgap boundaries; however, the upper limit of the trivial bandgap shows no dependence on the amplitude, remaining constant as the amplitude increases. Edge mode frequencies also increase with amplitude, some approaching the neighboring bulk bands at higher amplitudes. As they approach, edge modes eventually run tan-

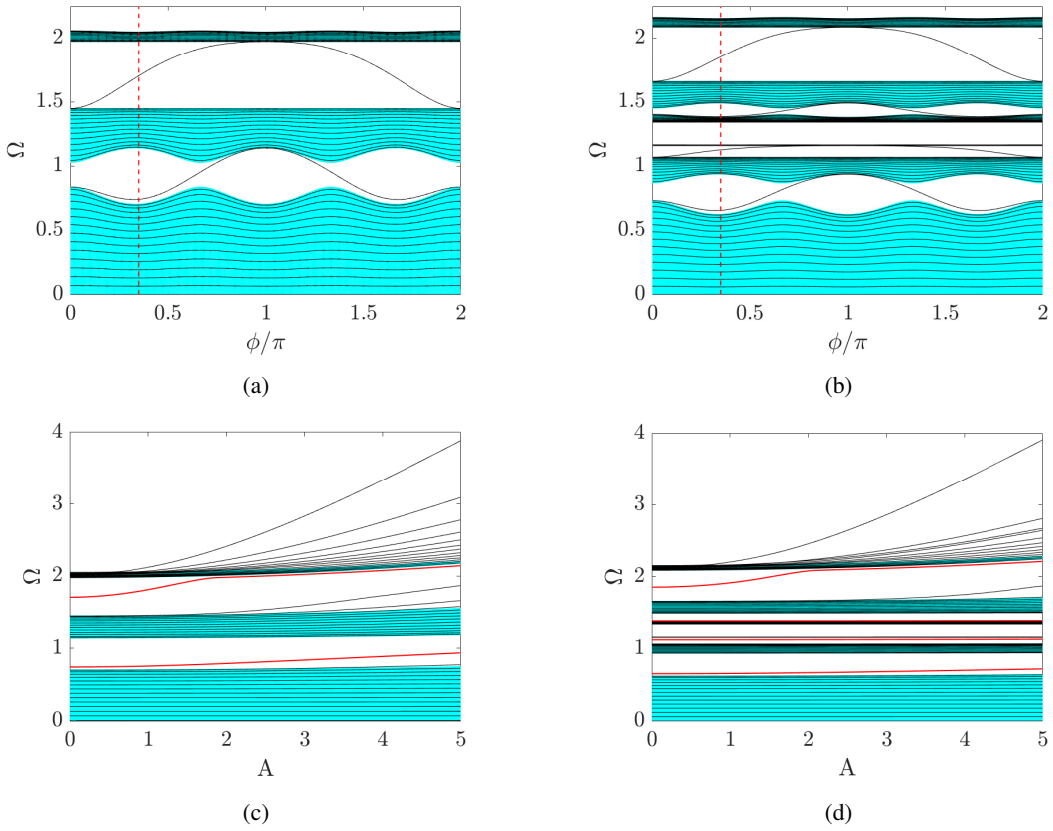


**FIGURE 2**: Effect of phase variable $\phi$ and excitation amplitude $A$ on dispersion relations. (a) Linear chain, without resonators; (b) Linear chain, with resonators; (c) Nonlinear chain, without resonators, $\phi = 0.35\pi$; (d) Nonlinear chain, with resonators, $\phi = 0.35\pi$.

gent to the band. While the majority of the finite chain modes remain within the infinite chain bulk bands, the highest modes in each band enter the bandgaps as amplitude increases and they are shifted to higher frequency. Previous works have shown that these modes, as well as the previously mentioned edge states, may display vibration localization [52]. Thus, the behavior of these modes is further investigated through the finite chain mode shapes acquired through harmonic balance.

### 3.2 MODE SHAPES

The effect of amplitude on the mode shapes of a nonlinear quasiperiodic chain without resonators is shown in Fig. 3. Mode shapes are normalized to the maximum displacement value for each amplitude, and the mode shapes for $A = 0.1$, 2.5, and 5 are outlined in black for clarity.

Three selected mode branches are shown here: the two edge states in Fig. 3(a) and (b) respectively, and the 41st mode in (c). The former two show that the edge modes result in localization to the ends of the chain. This localization is most pronounced at lower displacement amplitudes, where the effects of nonlinearity are negligible. However, as amplitude increases, the localization is affected to varying degrees. For the 1st edge mode in (a), increasing amplitude results in a more localized shape; while for the 2nd edge mode in (b), higher amplitude results in a less localized shape. This can be explained through the band structure in Fig. 2(c). Here, it is clear that while the 1st edge mode frequency increases with amplitude, it does not approach the 2nd pass band, remaining within the band gap even at the highest value of $A$. On the other hand, the 2nd edge mode does approach the 3rd pass band, running tangent to the band at increased amplitude. Thus, its behavior is more similar to the bulk band modes with less prominent localization. It can be concluded that localization is most significant when the mode frequency is within a bandgap and not approaching the edges. The phase $\phi$ will therefore have a significant impact on the effect of nonlinearity on mode shape localization, as it dictates the edge mode frequencies at low amplitude, and thus whether or not an edge mode will approach the next band with increasing amplitude.

Meanwhile, the 41st edge mode, shown in Fig. 3(c), begins within the 3rd pass band, then increases with amplitude to

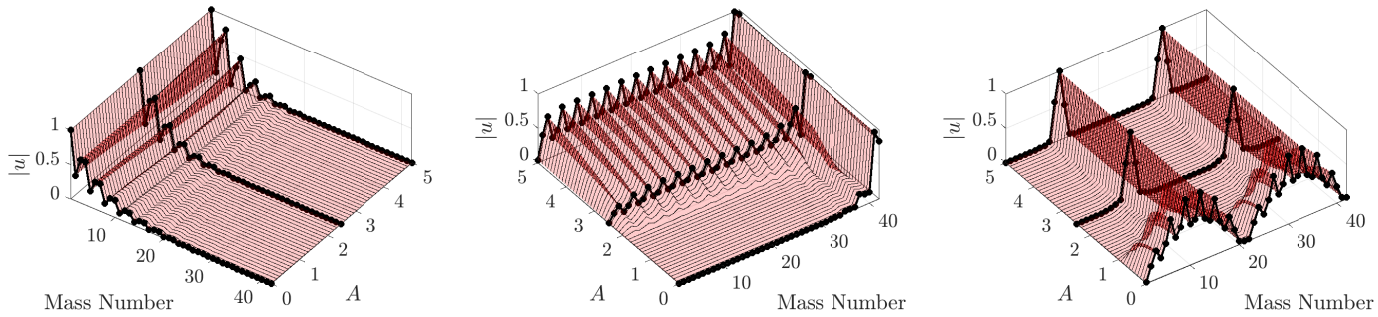


**FIGURE 3**: Effect of excitation amplitude $A$ on selected mode shapes of a nonlinear chain with $N = 42$ masses, without resonators, $\phi = 0.35\pi$. (a) 15th mode (1st edge mode); (b) 29th mode (2nd edge mode); (c) 41st mode.

enter the band gap. Thus, its mode shape become more localized, similar to the 1st edge mode. This case also illustrates the localization of modes that begin at the upper edge of the pass bands and enter the bandgaps at higher amplitude. The resulting mode shapes are localized to various points in the chain, forming discrete breathers. Breathers, which are solutions localized in space and periodic with time, have been established in prior work to emerge as modes at the edge of the pass bands enter the nonlinear regime [52–54]. This is of particular interest in the 2nd bandgap, where localized edge states and discrete breathers are both present. Overall, these observations for the chain without resonators are consistent with the previous work by Rosa et al. [52].

With the addition of resonators, many of the previous observations are still applicable. Though the band structure is split into 6 bands rather than 3, the behavior of the 3 bands above and below the trivial bandgap is observed to follow similar patterns, with each set of bands corresponding to the 3 bands of the non-resonator case. However, there are some notable differences in the presence of resonators. To compare and contrast the effect of resonators and the behavior of bands 1-3 and 4-6, the mode shapes of selected modes with varying displacement amplitude are shown in Fig. 4. Displacements of the main cells are marked with red circles, while the resonators are marked with blue squares. All displacements are normalized to the maximum displacement of the main cells at each amplitude.

The response for bands 1-3 with resonators is shown in Fig. 4(a)-(c). The 1st and 2nd edge modes are shown in (a) and (b), respectively, while the 41st mode is shown in (c). In all modes, it is clear that the resonators have larger displacement amplitude relative to the main cells, and that the relative resonator amplitude increases slightly for higher amplitude. The resonator amplitude can also be observed to increase as the mode frequencies approach the trivial bandgap and thus the resonator natural frequency. The 1st edge mode is very similar to the case without resonator, with displacement localized to one end of the chain. The 2nd edge mode, shown in Fig. 4(b), is similar to the non-resonator case at low amplitude, however, localization does not decrease as amplitude increases. The continued localization even at high amplitude may be explained by the band structure in Fig. 2(d). Looking closely at the 2nd edge mode, it can be seen that while the frequency does increase with amplitude, it remains away from the bandgap boundary and does not reach the point where it approaches and runs tangent to the 3rd band as in the non-resonator case. Thus, its behavior does not shift toward the band behavior, and remains localized. The 41st mode in Fig. 4(c) also displays differences from the case with no resonator. While there are two clear peaks in the displacement, localization does not intensify as amplitude increases. This is due to the fact that, unlike the non-resonator case, the 41st mode frequency does not increase with amplitude, and the mode shape is similarly unaffected.

For bands 4-6, the 3rd and 4th edge modes are shown in Fig. 4(d) and (e), while the 83rd mode is shown in (f). Here, the displacement response is extremely similar to the case without resonator, including the formation of breathers in mode 83. Unlike bands 1-3, the displacement of resonators relative to the main cells varies. For the 3rd edge mode, resonator displacement is greater than main cell displacement, while for the other two modes, it is significantly less. This indicates that the resonator displacement decreases as we look at modes farther from the trivial bandgap, matching the behavior in the lower 3 bands. One major difference between bands 1-3 and 4-6 is that the edge modes for the lower 3 bands have the resonators moving in phase with the main cells, while the resonators are out of phase for the upper 3 bands. This is illustrated by Fig. 5, which shows mode shapes for the 1st and 3rd edge modes with low displacement amplitude. Further exploration of the chain with resonators confirms that all modes below the trivial bandgap, and thus below the resonator natural frequency, have resonators in phase with the main cells, while above the trivial bandgap, resonators are out of phase. This matches observations of a similar system studied by

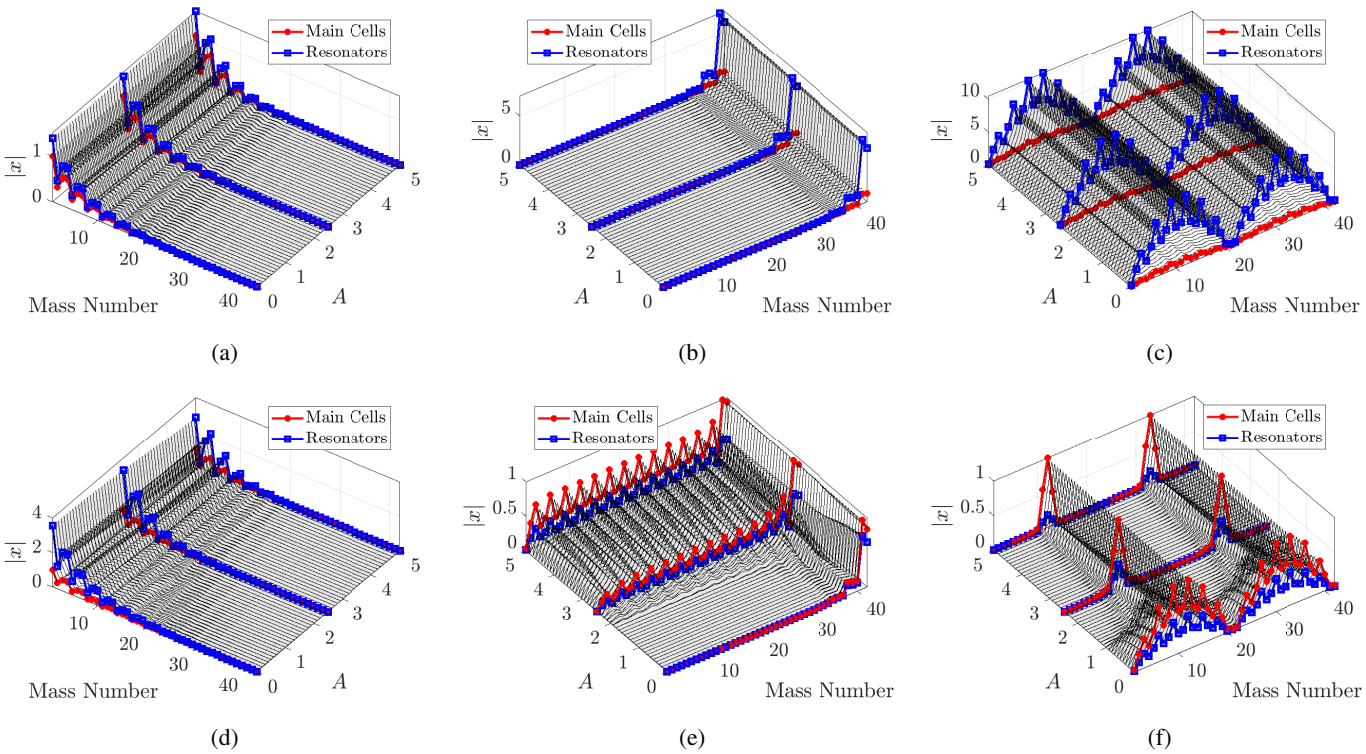


**FIGURE 4**: Effect of excitation amplitude $A$ on selected mode shapes of a nonlinear chain with $N = 42$ masses, with resonators, $\phi = 0.35\pi$. (a) 15th mode (1st edge mode); (b) 29th mode (2nd edge mode); (c) 41st mode; (d) 57th mode (3rd edge mode); (e) 71th mode (4th edge mode); (f) 83rd mode.

LeGrande et al. [55].

## 4 CONCLUSION

This work investigated the effect of incorporating local resonators into a nonlinear metamaterial with quasiperiodic stiffness modulation. The proposed system was modeled as a 1-dimensional lattice of masses connected by cubic nonlinear springs. Linear and nonlinear stiffness of the connecting springs was modulated following the Aubry-André Model. Each main mass was coupled to a local resonator also modeled as a spring-mass system. Multiple techniques were applied to study this nonlinear system, with the response of an infinite chain model solved analytically through the method of multiple scales and a the response of a finite chain estimated through the method of harmonic balance. The resulting frequency band structure and displacement mode shapes were compared to a similar system lacking local resonators to determine their effects.

In studying the proposed system, linear and nonlinear band structures were examined to determine the effects of phase variable and displacement amplitude. The results lacking resonator were found to be consistent with previous works, including the presence of nontrivial bandgaps, topological edge modes and amplitude dependence due to nonlinearity. With the addition of resonators, an additional trivial bandgap was observed, with nontrivial bandgaps appearing both below and above. The resulting bands below and above the trivial bandgap were shown to align closely with the bands of the system without resonators. The presence of topological edge modes in nontrivial bandgaps was demonstrated, but as expected, no edge mode appeared within the trivial bandgap. It was also observed that some modes near the upper edge of the pass bands shifted into the bandgaps as they entered the nonlinear regime.

The mode shapes of the system with and without resonator were also studied. Both with and without resonators, edge modes were shown to localize displacements to the ends of the chain. This localization was shown to change as edge modes entered the nonlinear regime. Modes that shifted deeper into the bandgaps showed increased localization, while edge modes that approached the edge of the pass bands showed decreased localization. Meanwhile, some non-edge modes shifted into the bandgaps as they entered the nonlinear regime, resulting in discrete breathers. Examining mode shapes also confirmed that in the presence of resonators, the bands above the trivial bandgap behaved almost identically to the bands of the non-resonator system. While also similar, the behavior of modes below the trivial

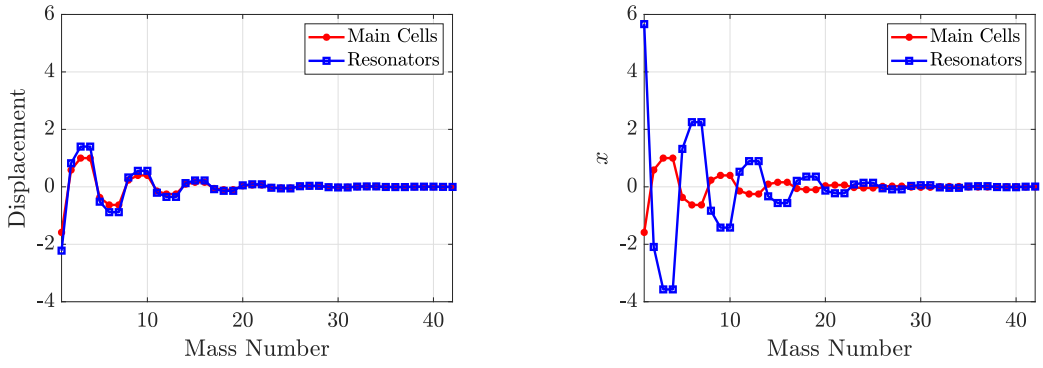


**FIGURE 5**: Selected mode shapes of nonlinear chain ($N = 42$) with resonators, $\phi = 0.35\pi$, $A = 0.1$. (a) Mode 15 (1st edge mode); (b) Mode 57 (3rd edge mode).

bandgap showed some differences to the non-resonator system. The displacement amplitude of resonators relative to the main cells was found to vary, with lower modes having resonator displacement greater than the main cells, while higher modes were the opposite. The phase of the local resonators was also found to be affected, with resonators being in phase with the main cells when below the trivial bandgap, and out of phase when above.

In conclusion, the addition of local resonators to a nonlinear, quasiperiodic metamaterial was shown to combine the effects of nonlinearity, stiffness modulation and local resonators with little conflict. Traits such as amplitude dependence and localized topological edge modes continued to manifest, and new bandgaps were added by the resonators. The resulting increase in number of edge modes, pass bands, and the presence of a trivial bandgap all serve to increase the versatility of the proposed metamaterial in both the linear and nonlinear regimes.

## ACKNOWLEDGEMENTS

This work is supported in part by the National Science Foundation (NSF) Grant CMMI-2038187.

## REFERENCES

[1] Bertoldi, K., Vitelli, V., Christensen, J., and van Hecke, M., 2017. "Flexible mechanical metamaterials". *Nature Reviews Materials,* ***2***(11), p. 17066.

[2] Hussein, M. I., Leamy, M. J., and Ruzzene, M., 2014. "Dynamics of phononic materials and structures: Historical origins, recent progress, and future outlook". *Applied Mechanics Reviews,* ***66***(4), p. 040802.

[3] Ma, G., and Sheng, P., 2016. "Acoustic metamaterials: From local resonances to broad horizons". *Science Advances,* ***2***(2), p. e1501595.

[4] Kivshar, Y., and Flytzanis, N., 1992. "Gap solitons in diatomic lattices". *Physical Review A,* ***46***(12), pp. 7972–7978.

[5] Liang, B., Yuan, B., and chun Cheng, J., 103. "Acoustic diode: Rectification of acoustic energy flux in one-dimensional systems". *Physical Review Letters,* ***46***, p. 104301.

[6] Cai, W., and Shalaev, V. M., 2010. *Optical Metamaterials*, Vol. 10. Springer.

[7] Christensen, J., Kadic, M., Kraft, O., and Wegener, M., 2015. "Vibrant times for mechanical metamaterials". *MRS Communications,* ***5***(3), pp. 453–462.

[8] Martínez-Sala, R., Sancho, J., Sánchez, J. V., Gómez, V., Llinares, J., and Meseguer, F., 1995. "Sound attenuation by sculpture". *Nature,* ***378***(6554), pp. 241–241.

[9] Achaoui, Y., Laude, V., Benchabane, S., and Khelif, A., 2013. "Local resonances in phononic crystals and in random arrangements of pillars on a surface". *Journal of Applied Physics,* ***114***(10), p. 104503.

[10] Sigalas, M. M., and Economou, E. N., 1992. "Elastic and acoustic wave band structure". *Journal of Sound and Vibration,* ***158***, pp. 377–382.

[11] Liu, Z., Zhang, X., Mao, Y., Zhu, Y., Yang, Z., Chan, C. T., and Sheng, P., 2000. "Locally resonant sonic materials". *Science,* ***289***(5485), pp. 1734–1736.

[12] Liu, L., and Hussein, M. I., 2012. "Wave motion in periodic flexural beams and characterization of the transition between bragg scattering and local resonance". *Journal of Applied Mechanics,* ***79***(1), p. 011003.

[13] Huang, G., and Sun, C., 2010. "Band gaps in a multiresonator acoustic metamaterial". *Journal of Vibration and Acoustics,* ***132***(3), p. 031003.

[14] Zhu, R., Liu, X., Hu, G., Sun, C., and Huang, G., 2014. "A chiral elastic metamaterial beam for broadband vibration suppression". *Journal of Sound and Vibration,* ***333***(10), pp. 2759–2773.

[15] Manimala, J. M., and Sun, C., 2016. "Numerical investigation of amplitude-dependent dynamic response in acoustic metamaterials with nonlinear oscillators". *The Journal of the Acoustical Society of America,* ***139***(6), pp. 3365–3372.

[16] Kivshar, Y. S., and Flytzanis, N., 1992. "Gap solitons in diatomic lattices". *Physical Review A,* ***46***(12), p. 7972.

[17] Nadkarni, N., Daraio, C., and Kochmann, D. M., 2014. "Dynamics of periodic mechanical structures containing bistable elastic elements: From elastic to solitary wave propagation". *Physical Review E,* ***90***(2), p. 023204.

[18] Popa, B.-I., Zigoneanu, L., and Cummer, S. A., 2011. "Experimental acoustic ground cloak in air". *Physical Review Letters,* ***106***(25), p. 253901.

[19] Farhat, M., Guenneau, S., and Enoch, S., 2009. "Ultrabroadband elastic cloaking in thin plates". *Physical Review Letters,* ***103***(2), p. 024301.

[20] Darabi, A., Zareei, A., Alam, M.-R., and Leamy, M. J., 2018. "Experimental demonstration of an ultrabroadband nonlinear cloak for flexural waves". *Physical Review Letters,* ***121***(17), p. 174301.

[21] Li, X.-F., Ni, X., Feng, L., Lu, M.-H., He, C., and Chen, Y.-F., 2011. "Tunable unidirectional sound propagation through a sonic-crystal-based acoustic diode". *Physical Review Letters,* ***106***(8), p. 084301.

[22] Ma, C., Parker, R. G., and Yellen, B. B., 2013. "Optimization of an acoustic rectifier for uni-directional wave propagation in periodic mass–spring lattices". *Journal of Sound and Vibration,* ***332***(20), pp. 4876–4894.

[23] Moore, K. J., Bunyan, J., Tawfick, S., Gendelman, O. V., Li, S., Leamy, M., and Vakakis, A. F., 2018. "Nonreciprocity in the dynamics of coupled oscillators with nonlinearity, asymmetry, and scale hierarchy". *Physical Review E,* ***97***(1), p. 012219.

[24] Nayfeh, A. H., 2011. *Introduction to Perturbation Techniques*. John Wiley & Sons.

[25] Nayfeh, A. H., and Mook, D. T., 2008. *Nonlinear Oscillations*. John Wiley & Sons.

[26] Narisetti, R. K., Leamy, M. J., and Ruzzene, M., 2010. "A perturbation approach for predicting wave propagation in one-dimensional nonlinear periodic structures". *Journal of Vibration and Acoustics,* ***132***(3), p. 031001.

[27] Manktelow, K., Leamy, M. J., and Ruzzene, M., 2011. "Multiple scales analysis of wave–wave interactions in a cubically nonlinear monoatomic chain". *Nonlinear Dynamics,* ***63***(1-2), pp. 193–203.

[28] Abedin-Nasab, M. H., Bastawrous, M. V., and Hussein, M. I., 2020. "Explicit dispersion relation for strongly nonlinear flexural waves using the homotopy analysis method". *Nonlinear Dynamics,* ***99***(1), pp. 737–752.

[29] Ganesh, R., and Gonella, S., 2013. "Spectro-spatial wave features as detectors and classifiers of nonlinearity in periodic chains". *Wave Motion,* ***50***(4), pp. 821–835.

[30] Zhou, W., Li, X., Wang, Y., Chen, W., and Huang, G., 2018. "Spectro-spatial analysis of wave packet propagation in nonlinear acoustic metamaterials". *Journal of Sound and Vibration,* ***413***, pp. 250–269.

[31] Bukhari, M., and Barry, O., 2019. "On the spectro-spatial wave features in nonlinear metamaterials with multiple local resonators". In ASME 2018 International Design Engineering Technical Conferences and Computers and Information in Engineering Conference, American Society of Mechanical Engineers.

[32] Bukhari, M., and Barry, O., 2020. "Simultaneous energy harvesting and vibration control in a nonlinear metastructure: A spectro-spatial analysis". *Journal of Sound and Vibration,* ***473***, p. 115215.

[33] Ma, G., Xiao, M., and Chan, C. T., 2019. "Topological phases in acoustic and mechanical systems". *Nature Reviews Physics,* ***1***(4), pp. 281–294.

[34] Mousavi, S. H., Khanikaev, A. B., and Wang, Z., 2015. "Topologically protected elastic waves in phononic metamaterials". *Nature Communications,* ***6***(1), pp. 1–7.

[35] Miniaci, M., Pal, R., Morvan, B., and Ruzzene, M., 2018. "Experimental observation of topologically protected helical edge modes in patterned elastic plates". *Physical Review X,* ***8***(3), p. 031074.

[36] Chaunsali, R., Chen, C.-W., and Yang, J., 2018. "Subwavelength and directional control of flexural waves in zone-folding induced topological plates". *Physical Review B,* ***97***(5), p. 054307.

[37] Rosa, M. I., Guo, Y., and Ruzzene, M., 2021. "Exploring topology of 1d quasiperiodic metastructures through modulated lego resonators". *Applied Physics Letters,* ***118***(13), p. 131901.

[38] Apigo, D. J., Qian, K., Prodan, C., and Prodan, E., 2018. "Topological edge modes by smart patterning". *Physical Review Materials,* ***2***(12), p. 124203.

[39] Xia, Y., Erturk, A., and Ruzzene, M., 2020. "Topological edge states in quasiperiodic locally resonant metastructures". *Physical Review Applied,* ***13***(1), p. 014023.

[40] LeGrande, J., Bukhari, M., and Barry, O., 2023. "Effect of electromechanical coupling on locally resonant quasiperiodic metamaterials". *AIP Advances,* ***13***(1), p. 015112.

[41] Ni, X., Chen, K., Weiner, M., Apigo, D. J., Prodan, C., Alù, A., Prodan, E., and Khanikaev, A. B., 2019. "Observation of hofstadter butterfly and topological edge states in reconfigurable quasi-periodic acoustic crystals". *Communications Physics,* ***2***(1), pp. 1–7.

[42] Pal, R. K., Rosa, M. I., and Ruzzene, M., 2019. "Topological bands and localized vibration modes in quasiperiodic beams". *New Journal of Physics,* ***21***(9), p. 093017.

[43] Rosa, M. I., Pal, R. K., Arruda, J. R., and Ruzzene, M., 2019. "Edge states and topological pumping in spatially modulated elastic lattices". *Physical Review Letters,*

***123***(3), p. 034301.
[44] Pal, R. K., Vila, J., Leamy, M., and Ruzzene, M., 2018. "Amplitude-dependent topological edge states in nonlinear phononic lattices". *Physical Review E,* ***97***(3), p. 032209.
[45] Vila, J., Paulino, G. H., and Ruzzene, M., 2019. "Role of nonlinearities in topological protection: Testing magnetically coupled fidget spinners". *Physical Review B,* ***99***(12), p. 125116.
[46] Darabi, A., and Leamy, M. J., 2019. "Tunable nonlinear topological insulator for acoustic waves". *Physical Review Applied,* ***12***(4), p. 044030.
[47] Tempelman, J. R., Matlack, K. H., and Vakakis, A. F., 2021. "Topological protection in a strongly nonlinear interface lattice". *Physical Review B,* ***104***(17), p. 174306.
[48] Chaunsali, R., Xu, H., Yang, J., Kevrekidis, P. G., and Theocharis, G., 2021. "Stability of topological edge states under strong nonlinear effects". *Physical Review B,* ***103***(2), p. 024106.
[49] Snee, D. D., and Ma, Y.-P., 2019. "Edge solitons in a nonlinear mechanical topological insulator". *Extreme Mechanics Letters,* ***30***, p. 100487.
[50] Chaunsali, R., and Theocharis, G., 2019. "Self-induced topological transition in phononic crystals by nonlinearity management". *Physical Review B,* ***100***(1), p. 014302.
[51] Chen, B. G.-g., Upadhyaya, N., and Vitelli, V., 2014. "Nonlinear conduction via solitons in a topological mechanical insulator". *Proceedings of the National Academy of Sciences,* ***111***(36), pp. 13004–13009.
[52] Rosa, M. I., Leamy, M. J., and Ruzzene, M., 2022. "Amplitude-dependent edge states and discrete breathers in nonlinear modulated phononic lattices". *arXiv preprint arXiv:2201.05526*.
[53] Flach, S., and Willis, C. R., 1997. "Discrete breathers".
[54] Boechler, N., Theocharis, G., and Daraio, C., 2011. "Bifurcation-based acoustic switching and rectification". *Nature Materials,* ***10***(9), p. 665.
[55] LeGrande, J., Bukhari, M., and Barry, O., 2022. "Topological properties and localized vibration modes in quasiperiodic metamaterials with electromechanical local resonators". In International Design Engineering Technical Conferences and Computers and Information in Engineering Conference, Vol. 86311, American Society of Mechanical Engineers, p. V010T10A004.